UNCECOMP 2025
6th ECCOMAS Thematic Conference on
Uncertainty Quantification in
Computational Sciences and Engineering
M. Papadrakakis, V. Papadopoulos, G. Stefanou (eds.)
Rhodes Island, Greece, 15-18 June 2025

PREDICTING BUILDING OPERATIONAL ENERGY UNDER MATERIAL DEGRADATION AND CLIMATE UNCERTAINTY: A SENSITIVITY ANALYSIS

Anna Maria Koniari[1], Charalampos P. Andriotis[1], Simona Bianchi[1], Pablo G. Morato[1], Seyran Khademi[1], and Mauro Overend[1]

[1] Faculty of Architecture and the Built Environment, Delft University of Technology

Julianalaan 134, 2628BL, Delft
e-mail: {a.m.koniari, c.andriotis, s.bianchi, p.g.moratodominguez, s.khademi, m.overend}@tudelft.nl

Abstract

Building energy prediction models expedite performance assessment and assist in decision-making, from early-stage design to retrofit planning at single- or multi-building scales. However, the number of parameters involved in the energy performance evaluation often impede the prediction process requiring the assimilation of high-dimensional, uncertain input. This is compounded further at multi-building scale e.g. urban energy modelling, due to the increased complexity of evaluating diverse building geometries. While single-building sensitivity and uncertainty analysis is well-established for identifying the most influential input parameters and evaluate the uncertainty effects on energy demand, these are hard to generalize at multi-building scale which remains relatively unexplored. The present study advances existing research by applying a variance-based sensitivity analysis to assess the impact of varying (i) building façade layout, (ii) envelope thermal properties, (iii) envelope air tightness and (iv) building occupancy. The analysis is conducted for multiple buildings under two future climate variations, while also considering the degradation of material thermal properties. The latter is derived from known deterioration models for single-building uncertainty propagation, relying on experimental and simulated data. The approach is applied to a temperate oceanic climate with particular focus on the Dutch building stock, including a sample of buildings with diverse geometric characteristics in Rotterdam. First-order Sobol indices are computed to evaluate the impact with respect to the heating, cooling and total energy demand. Our findings indicate that infiltration is the most influential factor for heating energy demand, whereas cooling is mostly affected by the envelope thermal properties and, particularly, window solar heat gain coefficient. Common patterns regarding the impact of insulation across different envelope components can be identified among buildings with similar orientation and compactness ratio indicating the importance of considering these geometric properties in retrofit decision-making workflows.

Keywords: sensitivity analysis, uncertainty propagation, building energy performance, climate change, material degradation.

1 INTRODUCTION

One third of the global energy consumption currently stems from the operational energy needs of buildings [1], making the building industry a key sector in the efforts to reduce carbon emissions. Energy upgrading of the building stock is essential since, in the EU, 80% of the current buildings is expected to be still in place by 2050 [2], but most of them are currently energy inefficient [3]. Moreover, ageing degradation of insulation is expected to cause long-term decay in thermal performance of the building envelope [4, 5], thus influencing the building energy performance [6]. In this direction, retrofit decision-making frameworks are needed to achieve maximum energy efficiency considering multi-faceted criteria [7]. These often rely on high-fidelity simulators and surrogate models for energy performance prediction [8], requiring a multitude of input parameters and associated uncertainties that can be hard to obtain [9].

Therefore, sensitivity analysis (SA) studies have been developed to identify the most impactful parameters for energy demand [10].

So far, the research has revolved around building sub-systems such as the building envelope or single-buildings [9, 11], while few SA studies examine the impact on diverse geometries [12] and urban-scale applications [13, 14]. Besides building-specific parameters [9], the effect of weather has also been evaluated, examining different locations [9, 12] or future climate scenarios [15, 16, 17]. Particularly, in cold climates, conventional overinsulating solutions, such as improving wall insulation or installing triple-glazed windows, can prove to be unsuitable in the future, since they can increase overheating risk during summer [18, 19] because of the expected increase in outside temperature due to climate change [20].

From a methodological perspective, SA studies for building energy performance analysis (BEPA) employ both local and global SA techniques, with global techniques being mostly preferred since they allow to explore the entire input space [21]. The most common GSA methods in BEPA are: (i) Morris method [22], which provides a qualitative ranking [13]; (ii) Sobol indices [23], which quantify the relative impact of the input parameters on the output [13]; (iii) hybrid approaches, using Morris method to screen out non-important parameters followed by the Sobol indices computation [9]. Sampling is usually conducted using Monte-Carlo sampling; Latin Hypercube Sampling (LHS) [9]; or Sobol sequence via the Saltelli scheme [13, 24].

In the Netherlands, given that heating outweighs cooling demand because of the cold climate, SA studies have primarily focused on evaluating the most influential parameters for heating energy demand using the standardized rank regression coefficient method [25, 26]. Moreover, evaluation of the impact of the total heating and cooling demand, as calculated according to the Dutch standards, has been conducted using Morris and Sobol methods [27]. The effect of insulation degradation on building energy performance has, however, not yet been examined in the Dutch context.

Focusing on the Dutch building stock, this study performs SA to examine the relative importance of building envelope and occupant-related parameters on both heating and cooling annual energy needs individually as well as in the total annual energy outcome. The study expands existing knowledge by identifying common patterns among different outputs and evaluates how these change in future weather conditions. Global sensitivity analysis (GSA) is employed to effectively explore the entire input space and, particularly, first-order Sobol indices are computed to allow for a quantitative comparison among input parameters. Diverse building geometries in Rotterdam are used to further examine how geometric characteristics affect both the Sobol indices and the distribution of the energy results. Moreover, material degradation uncertainties are considered during sampling. The energy results from all model evaluations are compared with the respective results at a pristine state to evaluate the effect of ageing in the energy demand. Overall, key insights are drawn regarding the impact of relevant parameters

and parameter groups on the energy outcome given current and future weather conditions; the effect of geometric characteristics on the parameter ranking; as well as the influence of material degradation in the energy demand in the Dutch context.

2 METHODOLOGY

The sensitivity analysis study is conducted on four existing single-family buildings of Rotterdam, capturing different adjacency types, size, layout and orientation (Table 1). The research methodology is structured into three main parts: (i) selection of example buildings; (ii) identification of input parameters; and (iii) sensitivity analysis (Fig.1).

Table 1: Geometric characteristics of example buildings. (AT: adjacency type (-) ; NF: number of floors (-); A_BF: total building floor area (m^2); AZ_EW: average azimuth of exposed walls (º); CR: compactness ratio (-); FH: floor height (m); A_EW: area of exterior walls (m^2); A_R: area of roof (m^2))

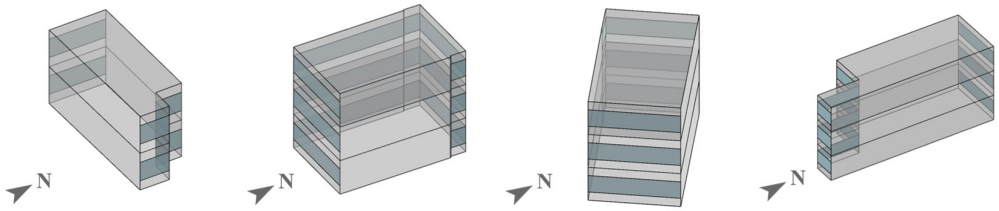

	Building 0 **(B0)**	Building 1 **(B1)**	Building 2 **(B2)**	Building 3 **(B3)**
AT	Terraced	Corner	Terraced	Terraced
NF	2	3	3	3
A_BF	93.90 m^2	190.62 m^2	138.58 m^2	179.70 m^2
AZ_EW	163.59º	179.65º	232.08º	151.64º
CR	1.67	1.73	1.24	1.17
FH	2.98 m	2.81 m	2.22 m	2.24 m
A_EW	62.48 m^2	203.37 m^2	80.06 m^2	90.81 m^2
A_R	46.95 m^2	63.54 m^2	46.19 m^2	59.90 m^2

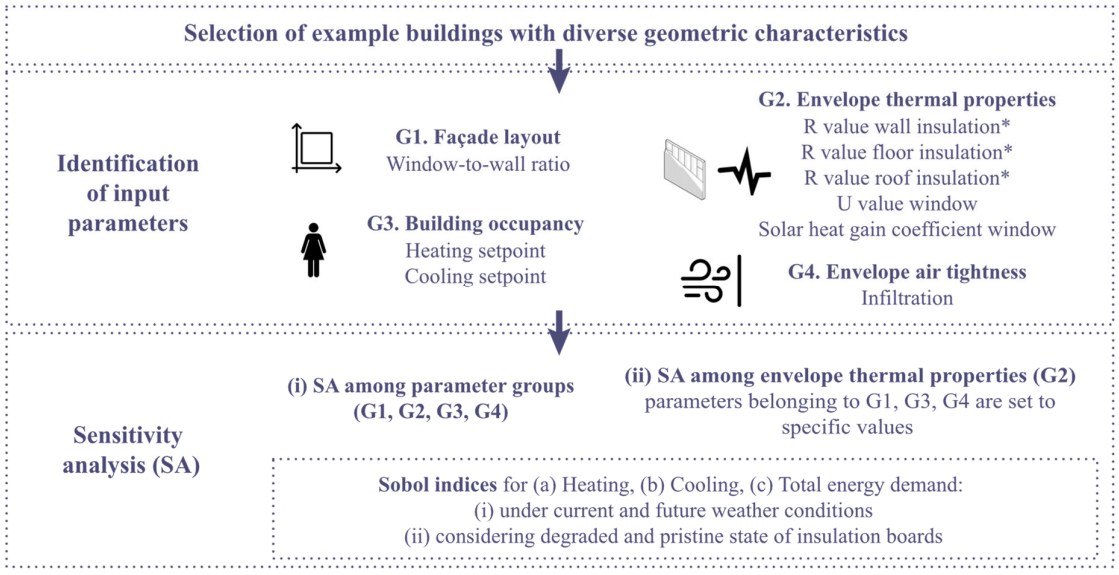

Figure 1:Schematic sensitivity analysis workflow. Input variables marked with an asterisk are calculated considering the degradation effect on insulation performance.

2.1 Selection of example buildings

Specifically, the example buildings consist of terraced houses (B0, B2, B3), which are situated in a row between two neighboring geometries, and a corner house (B1), which is placed at the end of the row and has only one adjacent building. The exposed walls and openings of B0, B2, B3 are in different orientations, with B0 being aligned in the east-west axis; B3 in the north-south; and B2 having an intermediate orientation, with exposed walls placed in south-east and north-west directions. Moreover, although B3 and B2 have the largest and second-largest total building floor area respectively, they are also the most compact when compared to B0, given their relatively smaller floor height. Lastly, unlike the other 3 buildings, B1 has only one neighboring building on the east side and all other wall surfaces are exposed to exterior weather conditions. Given the large area of exposed envelope surfaces, B1 is the least compact building, while, additionally, it has the largest total floor area of all example buildings.

2.2 Simulation setup

The building energy performance simulations are conducted using EnergyPlus [28] and the respective input data files (.idf) are generated using Eppy [29] and GeomEppy [30] Python libraries. All buildings correspond to single-family dwellings without individual apartments on each level. Therefore, although different thermal zones per floor are considered in the simulation, the final energy outcome is computed from the cumulative sum of the energy across all floors normalized by the total building floor area.

The building geometries are reconstructed in LoD (Level of Detail) 1.2, i.e. assuming a uniform volume extrusion with planar roofs and no height variations, using open-source data from the 3DBAG dataset [31]. Due to unavailability of data related to façade layout, all openings are generated in a uniform way using the presumed window-to-wall ratio. Specifically, they are created as horizontal openings in all walls that are exposed to exterior weather conditions.

Adiabatic conditions are assumed for interior floors, ceilings and wall surfaces that are adjacent to neighboring buildings, while all other surfaces are modelled as exposed to exterior conditions. Under the ground floor slab, the soil temperature is set to 18ºC throughout the year. This reflects the special case of soil under a conditioned slab, avoiding any extreme ground temperatures that can result in misleading building losses [32]. The effect of shading from neighboring buildings is not taken into account in the simulations. Lastly, mechanical ventilation is not considered and an ideal system with infinite capacity is assumed instead.

The computations follow the Dutch standards [33], which define that heating demand is evaluated only between October-March, while cooling is assessed between April-September. The annual total energy demand is the sum total of annual heating and cooling energy needs. Two different weather conditions are evaluated in the sensitivity analysis study; current and future weather variations (Fig.2). Specifically, the Typical Meteorological Year (TMY) weather file for Rotterdam-The Hague [34] is selected to represent current weather conditions, capturing interannual variability in the climate input. Future weather data are generated by applying the morphing technique through the future weather generator [35]. In this case, the TMY data are used as base to perform the morphing according to SSP 5-8.5 as defined from EC-Earth-3 climate model [36] for year 2050, indicating a worst-case scenario in which the rate of carbon emissions is not reduced in the long-term. Due to the nature of the morphing technique, which generates future data through adding or multiplying on top of historical weather values, trends in weather patterns are assumed to be maintained in future periods (Fig.2).

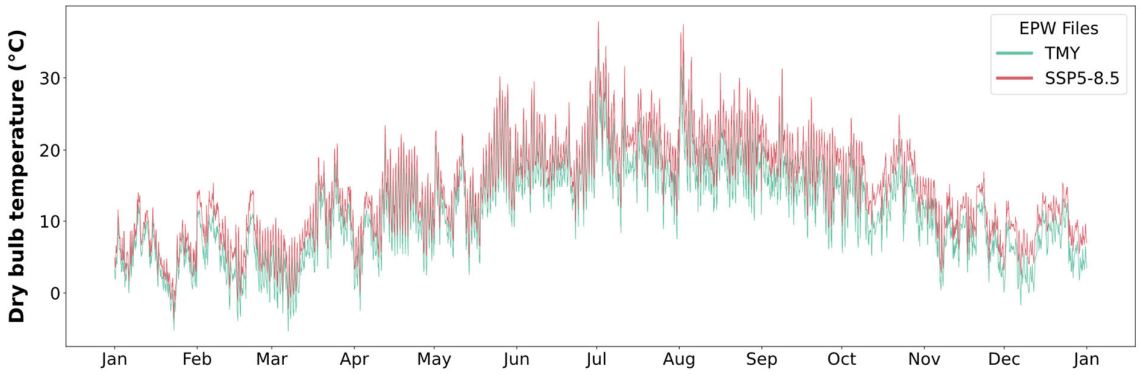

Figure 2: Hourly dry bulb temperature patterns for Rotterdam-The Hague during the course of a year according to TMY and SSP 5-8.5 data.

2.3 Sensitivity analysis setup

The input parameters X_i that are considered during sampling as well as their probabilistic distributions are defined based on literature and belong to the following groups (Table 2):

G_1. Façade layout. The variations in this group are expressed through window-to-wall (WWR) ratio (X_1) uncertainties. Given the use of existing buildings in this study, all other geometric characteristics, such as building layout, orientation and size, are extracted from open-source GIS data [31]. However, the distribution of openings in the façade is not directly available and, thus, assumptions are made regarding the WWR. In this study, the ranges used for the probabilistic distributions vary for terraced and corner houses and are based on information extracted from the Energy module of Woon2018 survey [37] and presented in [38].

G_2. Envelope thermal properties, including the thermal resistance (R value) of the insulation in opaque envelope components, i.e. wall (X_{2a}), roof (X_{3a}) and ground floor (X_{4a}); the effect of ageing in the thermal conductivity of insulation boards (X_{2b}, X_{3b}, X_{4b}); the thermal conductivity (U value) and solar heat gain coefficient (SHGC) of window glazing (X_5, X_6).

Apart from the ageing factor, the probabilistic distributions for all envelope thermal properties are uniform with minimum and maximum values defined based on typical archetype values [39] and potential retrofits designated particularly for the Dutch housing stock [40]. Specifically, in the case of insulation for opaque envelope components, the retrofits represent polyisocyanurate (PIR) insulation panels with varying material thicknesses. The minimum threshold of 2.7 m^2K/W (corresponding to the thermal resistance of an insulation board with thickness 80 mm) is further adjusted to 0.1 in (X_{2a}, X_{3a}, X_{4a}), capturing the possibility of the envelope components being uninsulated. Lastly, window thermal conductivity (U) values span a range from vacuum glazing to triple, double, and single glazing, while solar heat gain coefficient values do not consider the effect of shading and cover a range from clear single glazing to triple glazing with low-emissive coating.

The ageing factor is calculated accounting for an operation period of 20 years. By accounting for different weather files in the evaluation, the study captures both the option of buildings that were retrofitted in the past and have aged and the option of buildings being retrofitted today and aging over the next 20 years. In both cases, the ageing factor is defined following the approach described in [5].

$$d_{ins,20} \sim \mathcal{N}\left(\hat{d}_{ins,20}, \frac{\hat{d}_{ins,20} - 1}{3}\right) \quad (1)$$

where $d_{ins,20}$ is the sampled ageing factor; and $\hat{d}_{ins,20}$ is the mean ageing factor at year 20, defined using the Agesim software [41]. In the software calculations, loss of thermal performance in PIR insulation boards results only from alterations in gas phase conduction due to progressive gas diffusion. The standard deviation of the distribution is defined as a function of the mean ageing factor, thus progressively increasing over time. The thermal resistance of the insulation $r_{i,20}$ at each envelope component i (i.e. floor, wall, roof) is computed as:

$$r_{i,20} = r_{init,i} \cdot \frac{1}{d_{ins,20}} \quad (2)$$

where $r_{init,i}$ is the thermal resistance of the insulation in the i component at a pristine state. Since the ageing factor is defined for thermal conductivity, which is inversely proportional to thermal resistance, the inverse fraction of the ageing factor is considered in the calculation.

G_3. Envelope air tightness, including only infiltration (X_7) without accounting for uncertainties in natural ventilation schedules. Similarly to the thermal parameters, the interval of the uniform distribution is determined based on typical archetype values and potential retrofit interventions.

G_4. Building occupancy. The parameters here express uncertainties around the fixed values of heating and cooling thermostat setpoints (X_8, X_9), which can occur as a result of the building operation schedule.

Table 2: Random variables and probabilistic distributions employed in sensitivity analysis study.

Group	Variable	Distribution	Unit	Reference
G_1. Façade layout	X_1.Window-to-wall ratio	Uniform (Range: 0.43-0.66 for terraced houses, 0.20-0.30 for detached & corner houses	-	[38]
G_2. Envelope thermal properties	X_{2a}. R value of wall insulation at pristine state	Uniform (Range: 0.1-8.3)	m^2K/W	[40]
	X_{2b}. Ageing factor of wall insulation after 20 years	Normal (μ: 1.243, σ: 0.081)	-	[5]
	X_{3a}. R value of roof insulation at pristine state	Uniform (Range: 0.1-8.3)	m^2K/W	[40]
	X_{3b}. Ageing factor of roof insulation after 20 years	Normal (μ: 1.243, σ: 0.081)	-	[5]
	X_{4a}. R value of ground floor insulation at pristine state	Uniform (Range: 0.1-5.7)	m^2K/W	[40]
	X_{4b}. Ageing factor of ground floor insulation after 20 years	Normal (μ: 1.243, σ: 0.081)	-	[5]
	X_5. U value of window glazing	Uniform (Range: 0.6-2.9)	W/m^2K	[40, 42]
	X_6. Solar heat gain coefficient of window glazing	Uniform (Range: 0.5-0.9)	-	[13, 15, 27]
G_3. Envelope air tightness	X_7. Infiltration	Uniform (Range: 0.0004-0.003)	$\frac{m^3}{s \cdot m^2}$	[38, 39]
G_4. Building occupancy	X_8. Heating setpoint	Normal (μ: 20, σ: 0.7)	$°C$	[33, 43]
	X_9. Cooling setpoint	Normal (μ: 24, σ: 0.7)	$°C$	[33, 43]

2.4 First-order Sobol indices calculation

The sensitivity study is conducted into two phases: (i) assessing the impact of each parameter group $G_1 - G_4$ through grouped sampling and (ii) evaluating the relative impact of the individual envelope thermal parameters $X_{2a} - X_6$ when the input variables belonging to all other groups (G_1, G_3, G_4) are fixed. Specifically, in the second case, WWR and thermostat setpoints are fixed to the mean values of their probabilistic distributions, whereas infiltration is set to a slightly improved value, corresponding to a retrofit of crack sealing ($0.0007\ m^3/(s \cdot m^2)$) [38]. In this regard, the importance of interventions in the different envelope components is isolated and insights can be drawn on which interventions are important for retrofit decision-making workflows in order to mitigate heating, cooling and total energy needs. In each opaque envelope component, i.e. wall, roof and ground floor, values for insulation thermal resistance and ageing factor are grouped together during sampling and, thus, first-order Sobol indices are assigned per component (X_2, X_3, X_4).

In this study, sampling and first-order Sobol indices computation are conducted using the SALib Python library [44]. Specifically, sampling is performed using Sobol sequence [23] via the Saltelli scheme [24] to improve input space coverage. The total number of model evaluations for each building is defined as $N(2k + 2)$, where N corresponds to the number of samples and k corresponds to the number of sampling variables and/or groups, following the approach described in [45]. Due to computational time restrictions, 1,024 samples are drawn for each building in each of the two phases. Subsequently, 10,240 model evaluations are conducted per building in the case of grouped sampling ($k = 4$), and 12,288 model evaluations in the second phase, when only envelope thermal properties are assessed ($k = 5$). Confidence intervals are calculated using bootstrapping in order to assess the precision of the estimated values.

The relative impact of each input variable is evaluated using first-order Sobol indices which are computed following the approach described in [24]. Total-order Sobol indices are not presented in this study, since the higher-order interactions among variables proved to be negligible. The first-order Sobol index S_i for each variable X_i is defined as:

$$S_i = \frac{V_{X_i}(E_{\boldsymbol{X}_{\sim i}}(g(\boldsymbol{X}) \mid X_i))}{V\,[g(\boldsymbol{X})]} \tag{3}$$

where $g(\boldsymbol{X})$ is the output function; $E_{\boldsymbol{X}_{\sim i}}(g(\boldsymbol{X}) \mid X_i)$ is the expected value of the output function with respect to all input variables except X_i when X_i is fixed; $V_{X_i}(E_{\boldsymbol{X}_{\sim i}}(g(\boldsymbol{X}) \mid X_i))$ is the variance of the expected value when different values of X_i are assessed; and $V\,[g(\boldsymbol{X})]$ is the total variance of the output function. In this study, three main output functions are considered $g_h(\boldsymbol{X})$, $g_c(\boldsymbol{X})$ and $g_t(\boldsymbol{X})$, which represent the annual heating, cooling and total building energy demand respectively. All values are normalized with respect to the total building floor area.

3 RESULTS

The first-order Sobol indices (SIs) showing the impact of the different parameters and parameter groups along with the 95% confidence intervals are illustrated in Fig.3. Moreover, Fig.4 demonstrates the first-order Sobol indices computed for the variables belonging to G_2 without considering material degradation. Lastly, Fig. 5 shows a summary of the distribution of energy results among all model evaluations per building, while Fig. 6 provides a comparative analysis between the energy results corresponding to degraded and pristine material state.

When examining the influence of different parameter groups, it is observed that envelope air tightness (G_3) has the largest impact on both heating and total energy demand. In contrast, cooling is mostly affected by envelope thermal properties (G_2), followed by façade layout (G_1)

and air tightness (G_3) which are ranked equally. Building occupancy (G_4) has minor impact (SI < 0.15) in all buildings. Interestingly, the median and variance of cooling demand are significantly smaller than the heating and total energy demand distributions (Fig. 5).

In future weather conditions, the influence of all parameter groups ($G_1 - G_4$) on heating demand remains largely unchanged. However, the impact of envelope thermal properties (G_2) and façade layout (G_1) on cooling demand increases over time, resulting in their ranking as the highest and second-highest parameters, followed by building occupancy (G_4). The impact of envelope air tightness (G_3) on total energy demand also decreases in future weather conditions. In particular, the respective SIs show a greater reduction in B0 and B2, while in B1 it is maintained above 0.9. However, G_3 remains the most important parameter group in all buildings. This can be explained by the fact that heating remains overall larger than cooling demand regardless of the expected temperature increase due to climate change (Fig.4). Therefore, the parameters that influence heating remain the most influential for total energy demand as well. However, it can overall be observed that both median and variance of heating demand in future weather decrease when compared to current weather conditions, while the respective properties of cooling demand distributions increase in all buildings.

Although all buildings show uniform behavior in the grouped analysis, different patterns among example buildings can be observed in the second part of the study. Specifically, in current weather conditions, the heating demand of terraced houses (B0, B2, B3) is mostly influenced by the U value of window glazing (X_5), followed by the thermal resistance of roof (X_3) and wall (X_2) insulation respectively. However, X_2 becomes the most important feature in the case of B1, followed by the X_5 and X_3. In contrast, the cooling demand in all buildings is driven primarily by the solar heat gain coefficient of window glazing (X_6). The second most important parameter for cooling is X_5 for terraced houses and X_2 in the case of B1. Unlike heating which is not affected at all by the thermal resistance of the ground floor insulation (X_4), X_4 has a slight impact in cooling demand. However, X_3 does not affect at all the cooling energy outcome.

The observed trends vary in total energy demand. In buildings B0 and B2, X_6 is the most influential parameter, while X_3 and X_5 are the next most impactful variables. On the other hand, in B3, X_3 and X_5 are the most significant factors, with the third being X_6. This is likely due to the building orientation that leaves openings in the north and south sides, thus resulting in smaller impact of X_6 due to alterations in the solar heat gain that is received from the windows. In B1, X_2 has the largest SI, which can be explained by the larger area of exposed walls in this building (Table 1). X_4 has the lowest SI for total energy demand in all buildings.

Similar trends are repeated for heating and cooling in future weather conditions, with X_6 having an even larger impact on cooling compared to current weather conditions. Additionally, X_6 also becomes the determining factor for total energy demand in all terraced buildings, which can be explained by the fact that cooling almost outweighs heating in future conditions. Notably, B0 and B2, which have openings in east and west orientation, have the highest SI values for X_6. However, the SI for X_6 is smaller in the case B1 and almost matches the value of X_2, since the exposed wall area in this case is larger compared to the terraced houses. In fact, X_2 and X_4 are the least important parameter for total energy in B0, B2 and B3.

Comparing with the Sobol indices at the pristine state (Fig. 4), it can be observed that X_2 and X_3 have a larger impact on heating and total energy demand when degradation is considered. In contrast, X_5 and X_6 have overall larger impact in heating and total energy demand when all components are at their pristine state. All parameters have similar SIs in the case of cooling.

Notably, the variance of both heating and total energy demand are considerably smaller when infiltration is not varying, reflecting the large impact of this parameter in the outcome (Fig. 5). Moreover, the median of heating and total energy demand is decreased in all buildings

when compared to the grouped analysis, but cooling distributions remain almost unchanged. This reflects the small impact of infiltration in cooling demand, as demonstrated through the grouped analysis. In the analysis focusing on envelope thermal properties, total energy demand distributions remain roughly unchanged between current and future weather conditions, since the increase in cooling demand negates the reduction in heating due to climate change.

Lastly, in order to evaluate the effect of that insulation performance degradation on the energy outcome, the results of simulations with the same input values both with and without the degradation effect are compared. Afterwards, the ratio of the results at degraded state to the ones at pristine state is computed for each of the model evaluations in all buildings (Fig.6). Overall, total energy demand remains approximately unchanged in all cases. However, as a general pattern, heating energy is increased at the degraded state up to 8%, whereas cooling is decreased by up to 9%. The effect of degradation is in general small (< 10%), which is directly related to the fact that, in this study, only ageing due to gas diffusion in insulation of opaque envelope components is considered.

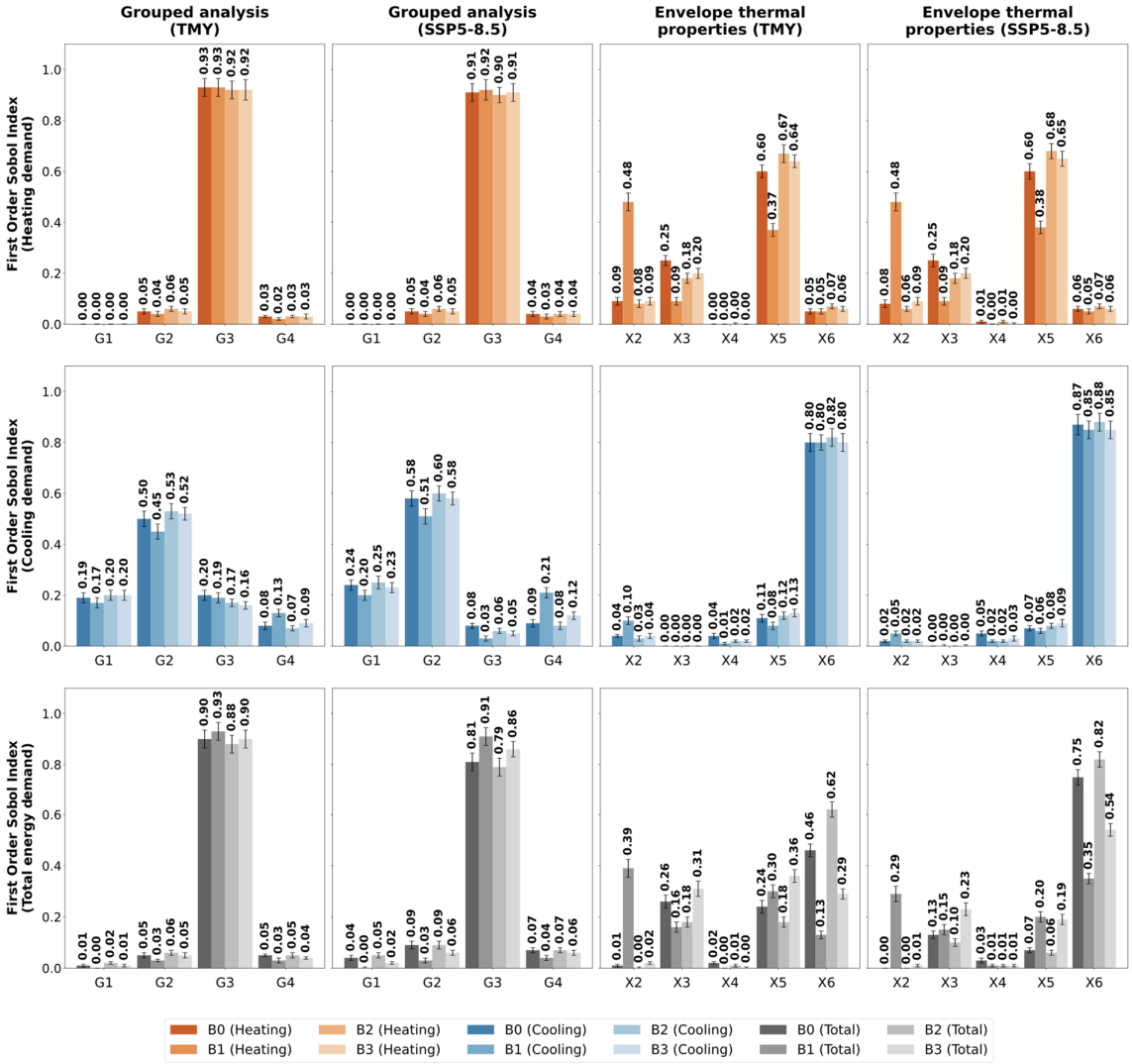

Figure 3: First-order Sobol indices showing the impact of distinct parameters and parameter groups in building heating, cooling and total energy demand under current (TMY) and future (SSP 5-8.5) weather conditions. The error bars represent the 95% confidence intervals computed via bootstrapping.

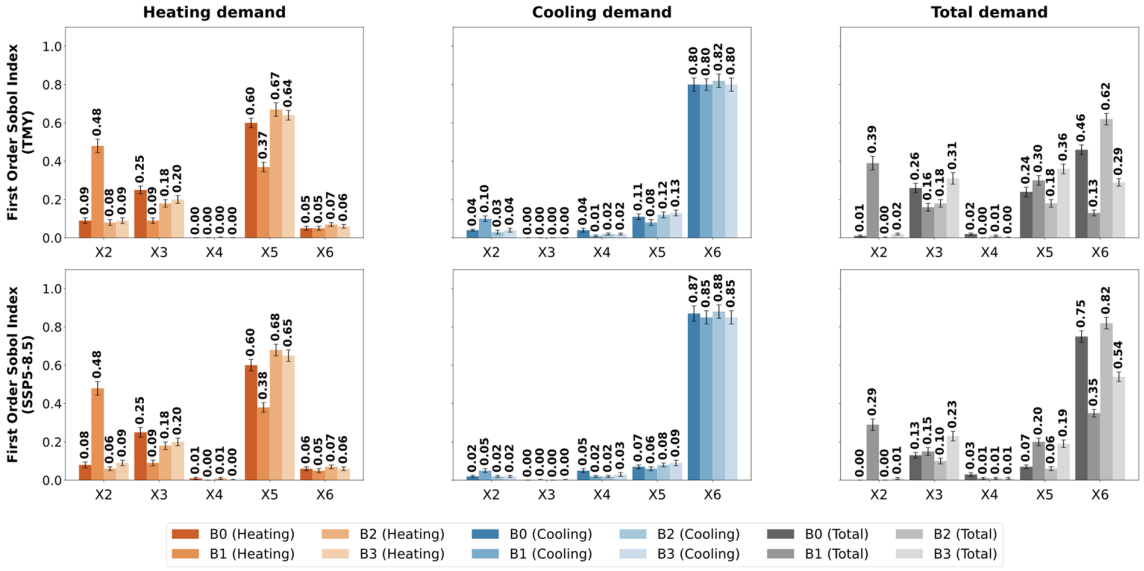

Figure 4: First-order Sobol indices showing the impact of the envelope thermal properties under current (TMY) and future (SSP 5-8.5) weather when all components are at pristine state. The error bars represent the 95% confidence intervals computed via bootstrapping.

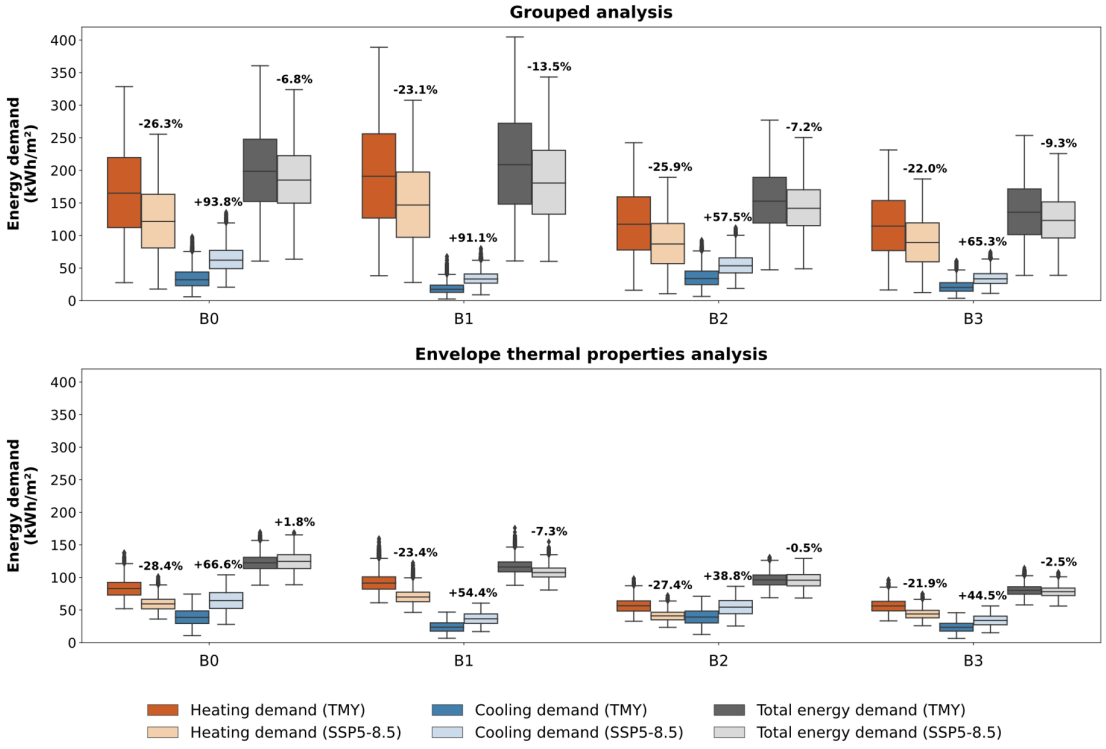

Figure 5: Distribution of heating, cooling and total energy demand results among all model evaluations per building. The boxes, whiskers and lines depict the minimum, first quartile, median, third quartile and maximum of the energy results distribution, showing the variance of the energy results at each SA run. The annotated percentages show the difference in the medians of each energy type between current and future weather conditions.

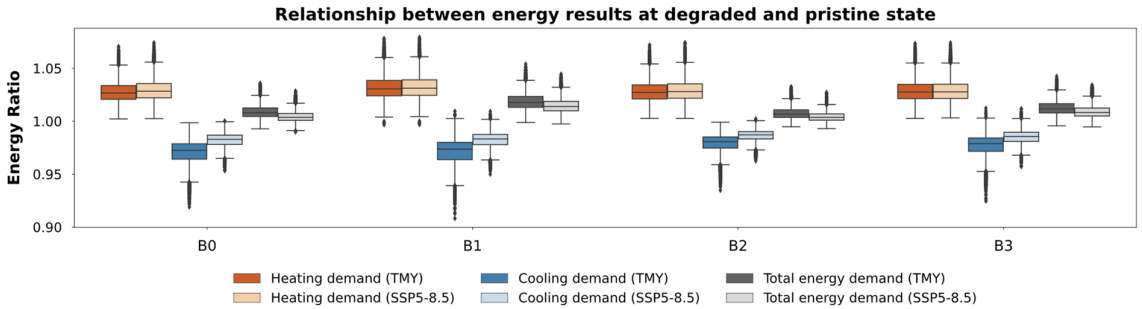

Figure 6: Ratio of heating, cooling and total energy demand at the degraded state with respect to the pristine state.

3.1 Discussion

The first part of the sensitivity analysis focuses on identifying which groups of input variables have the largest impact on heating, cooling and total energy demand in current and future weather conditions. Similarly to other results from literature [26], heating demand is primarily influenced by air infiltration. This result is due to increased air exchange which results in larger heat losses and, subsequently, increases the building heating demand. However, unlike other studies which show that temperature setpoints have a large influence on energy demand [12, 26], this study finds their effect to be marginal in all cases. This can be attributed to the probabilistic distributions used for sampling. In this study, normal distributions are used to assess the effect of uncertainty around the mean setpoint values, which are defined according to the Dutch standards [33]. However, in the other studies [12, 26], uniform distributions are used, evaluating how different setpoint values in an extended interval can affect the energy performance.

Moreover, it is worth emphasizing the change in Sobol indices between heating and cooling demand, given that the importance of input parameters for cooling demand in oceanic climates (mild winters and cool summers) is currently understudied. However, this will gain significant importance over time, given that the share of cooling to total energy demand increases in all cases. Particularly, the most important parameters for cooling are shown to be envelope thermal properties followed by window-to-wall ratio. The effect of infiltration is considerably lower in this case and decreases to an almost insignificant level for cooling demand in future weather. This is also seen from the fact that the median and variance of cooling demand are nearly identical in both grouped and envelope thermal properties analysis, when infiltration is kept constant. This result is directly linked to the way that infiltration is calculated in EnergyPlus [46] accounting for: (a) the stack effect, which occurs because of differences between interior and exterior air density due to temperature and moisture variations; and (b) the effect of wind speed. Both effects are expected to be lower during the summer period. This result is expected to change in the case that natural ventilation effect is taken into account in the simulations.

Although the trends change significantly for cooling, the Sobol indices for total energy demand follow similar patterns to the heating, because all example cases are heating dominated. However, the higher cooling demand in future weather conditions affects slightly the outcome and thus, infiltration is shown to have slightly lower Sobol indices in this case. The effect is particularly evident in B0 and B2 which are aligned to east/west and south-east/north-west directions respectively.

Besides the various differences in geometric properties of all 4 example cases, the ranges of total energy demand between buildings B0-B1 and B2-B3 are similar in both current and future weather scenarios. This is attributed to the similar values of compactness ratio in these pairs of buildings. This agrees with other studies where compactness ratio is shown to affect largely

heating demand in the Dutch context [26, 47]. Nonetheless, the share of cooling to total energy demand is larger in B0 and B2, which is presumably due to their orientation which is mostly aligned to the east/west axis. This is also reflected in these buildings having larger Sobol indices for solar heat gain coefficient and almost dominating cooling over heating energy demand in the detailed analysis in future climate conditions. As a general trend, the energy values for heating are reduced in all buildings in future conditions, whereas cooling demand increases by 38.8%-93.8%, when comparing the median values of the cooling energy distributions.

Besides compactness ratio, the total area of exposed walls also affects the outcome. In this regard, the wall R value is mostly important for B1, whereas in the case of terraced houses, U value of windows and R value of roof are overall more important. However, in this setup, the least influential parameter is the ground floor insulation. This can be linked to the way of simulation modelling, accounting for a constant soil temperature that reflects soil which is situated below a conditioned slab. Although window-to-wall ratio influences only cooling demand, it is considered as important given the increased value of cooling needs in future conditions. In heating demand, the SIs of WWR are surprising, given that the window U value is shown to influence heating in all cases in the second part of the analysis. However, the influence of infiltration is dominating in this case and, therefore, the relative impact of the other parameter groups may be affected accordingly.

Additionally, it is noteworthy that when infiltration, thermostat setpoints and window-to-wall ratio values are constant, the median and variance of energy demand in all buildings is considerably lower. Cooling energy in this case accounts for a larger proportion of the total energy demand and even outweighs heating in B0 and B2 in future weather conditions. Degradation of insulation performance has only small effects on the energy performance when compared to results with materials at pristine state, resulting in increased heating and decreased cooling energy demand because of lower thermal resistance of the building envelope. However, the effect on energy demand is only marginal, which is linked to the fact that, in this study, only ageing due to gas diffusion in insulation boards is considered. Other sources from uncertainty have also been mentioned in the literature, such as loss in effective area of insulation [5]; degradation of insulation performance due to moisture [48] and temperature differences [49]; and weakening of thermal conductivity due to loss of argon in windows [50]. Integrating the various sources of uncertainty in the energy-retrofit decision-making workflow is considered important to allow for a realistic evaluation of energy performance [7].

4 CONCLUSIONS

This study performs sensitivity analysis to identify the most important parameters among geometric, material and occupant-related criteria to include in energy assessment workflows. The study is performed in a temperate oceanic climate under current and future weather conditions to capture the expected shift in heating and cooling needs due to global warming. Among all example buildings, important features to integrate in energy prediction models are: (i) compactness ratio, which influences the total energy needs; (ii) window orientation and window-to-wall ratio, influencing primarily cooling demand. Uncertainties in temperature setpoints only have a marginal effect, unless sampled from uniform distributions that cover diverse human preferences. Overall, improving infiltration is found to be the most important retrofit in the given setup, because it impacts both heating and total energy demand, but its effect on cooling is small, especially in future climate conditions. In contrast, envelope thermal parameters are the most impactful factor for cooling energy demand. Building upon this, when the infiltration is set to a slightly improved value, both the median and variance of the heating and total energy distribution are significantly smaller, whereas cooling is increased, indicating a potentially higher risk of overheating during summer. In this case, heating is mostly affected by the window

U value for terraced and the wall insulation for the corner house, while window solar heat gain coefficient has the largest impact on cooling energy. Moreover, although roof insulation affects heating and total energy demand, it has minimal effect on cooling. Other patterns vary per building, indicating that it is important to consider geometric differences in urban energy retrofit decisions, unlike typical archetype classifications that are usually only based on building adjacency type and construction year. Notably, given fixed infiltration rate, window solar heat gain coefficient has larger impact in the total energy demand for east-west orientation, while wall insulation affects more the total energy in corner houses, given the larger wall area. Ground floor insulation has minimal effect in all cases. Lastly, long-term degradation of insulation performance due to gas diffusion modifies the building energy profile, but other sources of uncertainty should also be included to allow for more realistic energy outcome. Future research can conduct time-dependent sensitivity analysis to identify the importance of different degradation sources along the building lifecycle, incorporate natural ventilation effects and/or evaluate the results for different climate models and weather scenarios.

5 ACKNOWLEDGEMENTS

This material is based upon work supported by the DE-CIST project under the ICLEI Action Fund, the MultiCare EU project (GA no. 101123467), and the TU Delft AI Labs program.

6 REFERENCES

[1] IEA, "Tracking Clean Energy Progress 2023," IEA, Paris, 2023.

[2] World Economic Forum, "Transforming Energy Demand," 2024.

[3] European Union, "Directive (EU) 2024/1275 of the European Parliament and of the Council of 24 April 2024 on the energy performance of buildings (recast)," Official Journal of the European Union, 2024.

[4] D. A. Waddicor, E. Fuentes, L. Sisó, J. Salom, B. Favre, C. Jiménez and M. Azar, "Climate change and building ageing impact on building energy performance and mitigation measures application: A case study in Turin, northern Italy.," *Building and Environment,* vol. 102, 2016.

[5] Z. Liu, X. Zhou, W. Tian, X. Liu and D. Yan, "Impacts of uncertainty in building envelope thermal transmittance on heating/cooling demand in the urban context," *Energy and Buildings,* vol. 273, p. 112363, 2022.

[6] A. Taki and A. Zakharanka, "The Effect of Degradation on Cold Climate Building Energy Performance: A Comparison with Hot Climate Buildings," *Sustainability,* vol. 15, no. 8, p. 6372, 2023.

[7] W.-S. Yun, W. Ryu, D. Lee and H. Seo, "Energy-saving potential estimation of retrofitting aged buildings considering external wall insulation degradation," *Journal of Building Engineering,* vol. 94, p. 110022, 2024.

[8] C.-H. Park and C. S. Park, "Limitations and issues of conventional artificial neural network-based surrogate models for building energy retrofit," *Journal of Building Performance Simulation,* vol. 17, no. 3, pp. 361-370, 2024.

[9] Z. Pang, Z. O'Neill, Y. Li and F. Niu, "The role of sensitivity analysis in the building performance analysis: A critical review," *Energy and Buildings,* vol. 209, p. 109659, 2020.

[10] C. Carpino, R. Bruno, V. Carpino and N. Arcuri, "Improve decision-making process and reduce risks in the energy retrofit of existing buildings through uncertainty and sensitivity analysis," *Energy for Sustainable Development,* vol. 68, pp. 289-307, 2022.

[11] Q. Jin and M. Overend, "Sensitivity of façade performance on early-stage design variables," *Energy and Buildings,* vol. 77, pp. 457-466, 2014.

[12] A. Demir Dilsiz, K. Ng, J. Kämpf and Z. Nagy, "Ranking parameters in urban energy models for various building forms and climates using sensitivity analysis," *Building Simulation,* vol. 16, no. 9, pp. 1587-1600, 2023.

[13] M. Mosteiro-Romero, J. A. Fonseca and A. Schlueter, "Seasonal effects of input parameters in urban-scale building energy simulation," *Energy Procedia,* vol. 122, pp. 433-438, 2017.

[14] M. Y. C. Van Hove, M. Delghust and J. Laverge, "Uncertainty and sensitivity analysis of building-stock energy models: sampling procedure, stock size and Sobol' convergence," *Journal of Building Performance Simulation,* vol. 16, no. 6, pp. 749-771, 2023.

[15] A. J. Ibrahim, D. D. Zangana, S. Liu, H. Samuelson and L. Yang, "Impacts of climate change on energy-saving sensitivity of residential building envelope design parameters in three hot-dry cities," *Journal of Building Engineering,* vol. 99, p. 111481, 2025.

[16] R. Chen, H. Samuelson, Y. Zou, X. Zheng and Y. Cao, "Improving building resilience in the face of future climate uncertainty: A comprehensive framework for enhancing building life cycle performance," *Energy and Buildings,* vol. 302, p. 113761, 2024.

[17] S. Liu, Y. Wang, X. Liu, L. Yang, Y. Zhang and J. He, "How does future climatic uncertainty affect multi-objective building energy retrofit decisions? Evidence from residential buildings in subtropical Hong Kong," *Sustainable Cities and Society,* vol. 92, p. 104482, 2023.

[18] D. R. Liyanage, K. Hewage, S. A. Hussain, F. Razi and R. Sadiq, "Climate adaptation of existing buildings: A critical review on planning energy retrofit strategies for future climate," *Renewable and Sustainable Energy Reviews,* vol. 199, p. 114476, 2024.

[19] U. Y. Ayikoe Tettey and L. Gustavsson, "Energy savings and overheating risk of deep energy renovation of a multi-storey residential building in a cold climate under climate change," *Energy,* vol. 202, 2020.

[20] U. Berardi and P. Jafarpur, "Assessing the impact of climate change on building heating and cooling energy demand in Canada," *Renewable and Sustainable Energy Reviews,* vol. 121, p. 109681, 2020.

[21] W. Tian, "A review of sensitivity analysis methods in building energy analysis," *Renewable and Sustainable Energy Reviews,* vol. 20, pp. 411-419, 2013.

[22] M. Morris, "Factorial Sampling Plans for Preliminary Computational Experiments," *Technometrics,* vol. 33, no. 2, pp. 161-174, 1991.

[23] I. M. Sobol, "Global sensitivity indices for nonlinear mathematical models and their Monte Carlo estimate," *Mathematics and Computers in Simulation,* vol. 55, no. 1-3, pp. 271-280, 2001.

[24] A. Saltelli, P. Annoni, I. Azzini, F. Campolongo, M. Ratto and S. Tarantola, "Variance based sensitivity analysis of model output. Design and estimator for the total sensitivity index," *Computer Physics Communications,* vol. 181, pp. 259-270, 2010.

[25] A. Ioannou and L. Itard, "Energy performance and comfort in residential buildings: Sensitivity for building parameters and occupancy," *Energy and Buildings,* vol. 92, pp. 216-233, 2015.

[26] P. Wahi, T. Konstantinou, H. Visscher and M. J. Tenpierik, "Evaluating building-level parameters for lower-temperature heating readiness: A sampling-based approach to addressing the heterogeneity of Dutch housing stock," *Energy and Buildings,* vol. 322, p. 114703, 2024.

[27] M. Kafaei, "Sensitivity Analysis of NTA8800 for a Dutch Building Renovation Tendering System," 2021.

[28] National Renewable Energy Laboratory (NREL), *EnergyPlus™,* 2017.

[29] "Eppy," 2013. [Online]. Available: https://github.com/santoshphilip/eppy. [Accessed 12 03 2025].

[30] "GeomEppy," [Online]. Available: https://github.com/jamiebull1/geomeppy. [Accessed 12 03 2025].

[31] R. Peters, B. Dukai, S. Vitalis, J. Van Liempt and J. Stoter, "Automated 3D Reconstruction of LoD2 and LoD1 Models for All 10 Million Buildings of the Netherlands," *Photogrammetric Engineering & Remote Sensing,* vol. 88, no. 3, pp. 165-170, 2022.

[32] U.S. Department of Energy, "EnergyPlus version 24.2.0 Documentation Input Output Reference," 2024.

[33] S. K. N. N. Instituut, "Nederlandse technische afspraak NTA 8800:2024 Energieprestatie van gebouwen - Bepalingsmethode," 2024.

[34] "Climate-OneBuilding.Org," [Online]. Available: https://climate.onebuilding.org/. [Accessed 13 03 2025].

[35] E. Rodrigues, M. S. Fernandes and D. Carvalho, "Future weather generator for building performance research: An open-source morphing tool and an application," *Building and Environment,* vol. 233, p. 110104, 2023.

[36] R. Döscher, M. Acosta, A. Alessandri, P. Anthoni, T. Arsouze, T. Bergman, R. Bernardello, S. Boussetta, L.-P. Caron, G. Carver, M. Castrillo, F. Catalano, I. Cvijanovic, P. Davini, E. Dekker, F. J. Doblas-Reyes, D. Docquier, P. Echevarria, U. Fladrich, R. Fuentes-Franco, M. Gröger, J. v. Hardenberg, J. Hieronymus, M. Karami, J.-P. Keskinen, T. Koenigk, R. Makkonen, F. Massonnet, M. Ménégoz, P. A. Miller, E. Moreno-Chamarro, L. Nieradzik, T. van Noije, P. Nolan, D. O'Donnell, P. Ollinaho, G. van den Oord, P. Ortega, O. Prims, A. Ramos, T. Reerink, C. Rousset, Y. Ruprich-Robert, P. Le Sager, T. Schmith, R. Schrödner, F. Serva, V. Sicardi, B. Smith, Tian, T. Tian, E. Tourigny, P. Uotila, M. Vancoppenolle, S. Wang, D. Wårlind, U. Willén, K. Wyser, S. Yang, X. Yepes-Arbós and Q. Zhang, "The EC-Earth3 Earth system model for the Coupled Model Intercomparison Project 6," *Geoscientific Model Development,* vol. 15, no. 7, pp. 2973-3020, 2022.

[37] Woononderzoek Nederland, "WoON 2018".

[38] Rijksdienst voor Ondernemend Nederland, "Voorbeeldwoningen," 2022.

[39] Nieman De Raadgevende Ingenieurs, "Verduurzaming Rotterdamse woningvoorraad," 2023.

[40] [Online]. Available: https://regelhulpenvoorbedrijven.nl/kostenkentallen/. [Accessed 09 February 2025].

[41] S. N. Singh and P. D. Coleman, "Accelerated Aging Test Methods for Predicting the Long Term Thermal Resistance of Closed-Cell Foam Insulation," in *Center for Polyurethanes Industries Conference*, 2007.

[42] "TABULA WebTool," [Online]. Available: https://webtool.building-typology.eu/#bm. [Accessed 26 September 2024].

[43] G. Calleja Rodríguez, A. Carrillo Andrés, F. Domínguez Muñoz, J. M. Cejudo López and Y. Zhang, "Uncertainties and sensitivity analysis in building energy simulation using macroparameters," *Energy and Buildings,* pp. 79-87, 2013.

[44] J. Herman and W. Usher, "SALib: An open-source Python library for Sensitivity Analysis," *The Journal of Open Source Software,* vol. 2, no. 9, p. 97, 2017.

[45] A. Saltelli, "Making best use of model evaluations to compute sensitivity indices," *Computer Physics Communications,* vol. 145, no. 2, pp. 280-297, 2002.

[46] U.S. Department of Energy, "Engineering Reference (EnergyPlus Version 24.2.0 Documentation)," 2024.

[47] Nieman De Raadgevende Ingenieurs, "Rapport standaard en streefwaardes bestaande woningbouw," 2021.

[48] F. Tariku, Y. Shang and S. Moletti, "Thermal performance of flat roof insulation materials: A review of temperature, moisture and aging effects," *Journal of Building Engineering,* vol. 76, no. 2023, p. 107142.

[49] S. Moletti and D. Van Reenen, "Effect of Temperature on Long-Term Thermal Conductivity of Closed-Cell Insulation Materials," *Buildings,* vol. 12, no. 4, p. 425, 2022.

[50] S. K. Asphaug, B. P. Jelle, L. Gullbrekken and S. Uvsløkk, "Accelerated ageing and durability of double-glazed sealed insulating window panes and impact on heating demand in buildings," *Energy and Buildings,* vol. 116, pp. 395-402, 2016.